Supporting Information

Theoretical Study of Surface Dependence of NH_3 Adsorption and Decomposition on Spinel-type $MgAl_2O_4$

Huan Wang,[a] Chuanyi Jia,[b] Jing Yang,[a] Xian Zhao,[b] Yanlu Li,[b] Honggang Sun[c] and Weiliu Fan*[a]

a) School of Chemistry and Chemical Engineering, Shandong University, Jinan 250100 China

b) State Key Laboratory of Crystal Materials, Shandong University, Jinan 250100 China

c) School of Environmental Science and Engineering, Shandong University, Jinan 250100 China

*Corresponding author. E-mail: fwl@sdu.edu.cn

1. The choice of the number of slab layers:

The data in Table S1 showed that the convergence surface energies were conducted in different slab layers of three surfaces. According to the change in the data, we selected the proper slab layer for further NH_3 adsorption and reaction calculation.

Table S1. The Convergence Test for the Layers of (100), (110) and (111) Surfaces

Surface plane	Termination	Surface energy(eV/ Å^2)
(100)	5	0.11
	7	0.13
	9	0.15
(110)	5	0.16
	6	0.17
	7	0.18
(111)	5	0.14
	7	0.15
	9	0.16

2. The optimized configurations:

Based on the five models presented in Figure 2, several NH_3 molecule adsorption configurations on $MgAl_2O_4$ (100), (110) and (111) surfaces were calculated carefully and showed in Figure S1-3: the Initial Types represent the established surface slab structures without geometry optimization, and the Optimized Types represent the optimized structures.

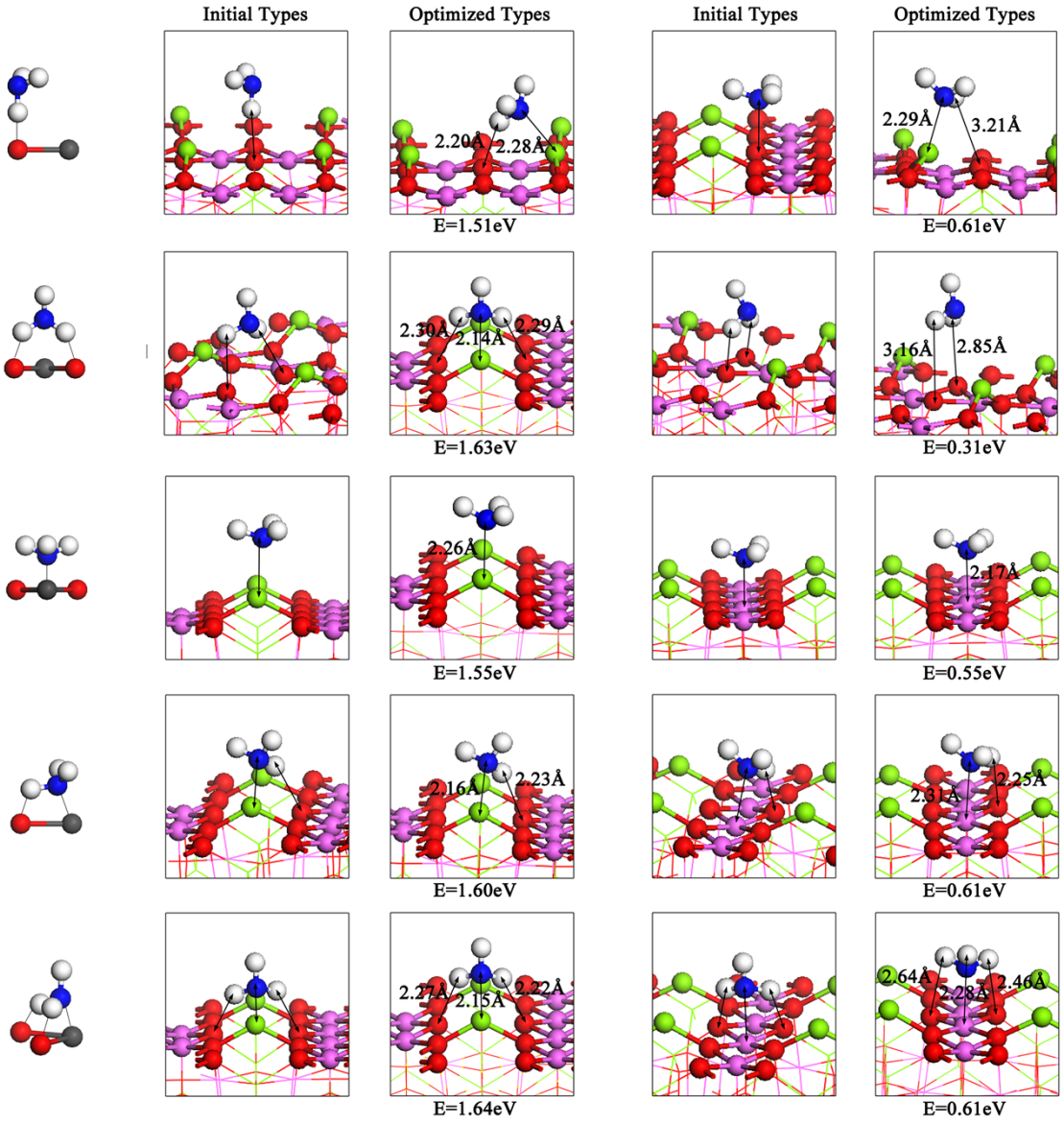

Figure S1. The Initial and Optimized Types of NH_3 molecule adsorption states on (100) surface on the basis of the five models.

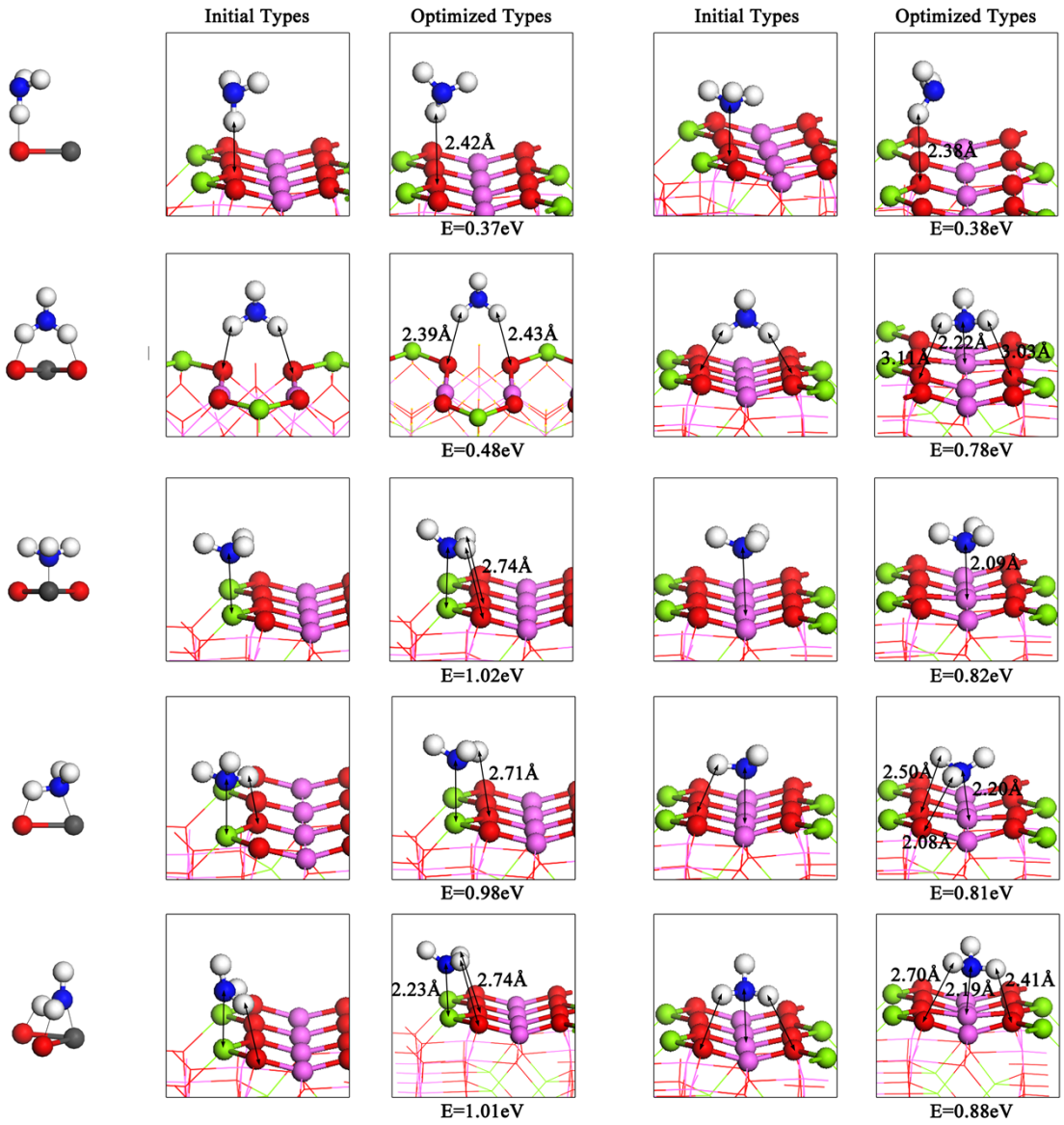

Figure S2. The Initial and Optimized Types of NH_3 molecule adsorption states on (110) surface on the basis of the five models.

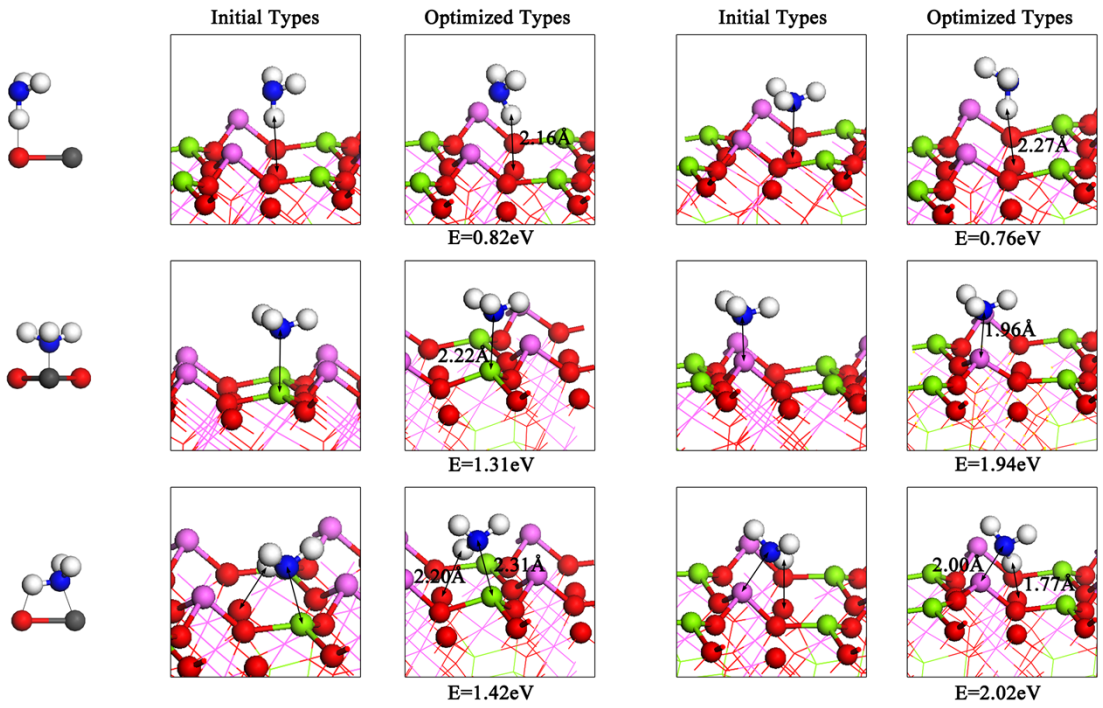

Figure S3. The Initial and Optimized Types of NH_3 molecule adsorption states on (111) surface on the basis of the five models.

3. The treatment of the surface polarity

Two $MgAl_2O_4$ surface slab models (Figure S4) were established to eliminate the polarity of the surface. One way was to build non-stoichiometric surface slab with the similar structure of upper and bottom surfaces; the other way was that the surface dangling bonds on the bottom layer of $MgAl_2O_4$ polar surface were saturated by hydrogen atoms. The two surface configurations were used to investigate the NH_3 adsorption behavior in comparison with the adsorption on polar surface seen in Figure S5-7. This paper primarily investigated the interaction between the NH_3 and surface sites, and the reaction mechanism of NH_3 dissociation. For (100) surface in Figure S5, it was easy to find the NH_3 adsorption on Mg_{2c} site was still the favorable adsorption sites in comparing the three types of surfaces. In addition, the NH_3 dissociation adsorption remained on Mg_{2c} site. Similarly, the surface polarity did not change the active sites and the NH_3 reaction process on (110) and (111) surface. Therefore, the results indicated that the polarity played little effect on the selectivity of surface active sites and the NH_3 dissociation process.

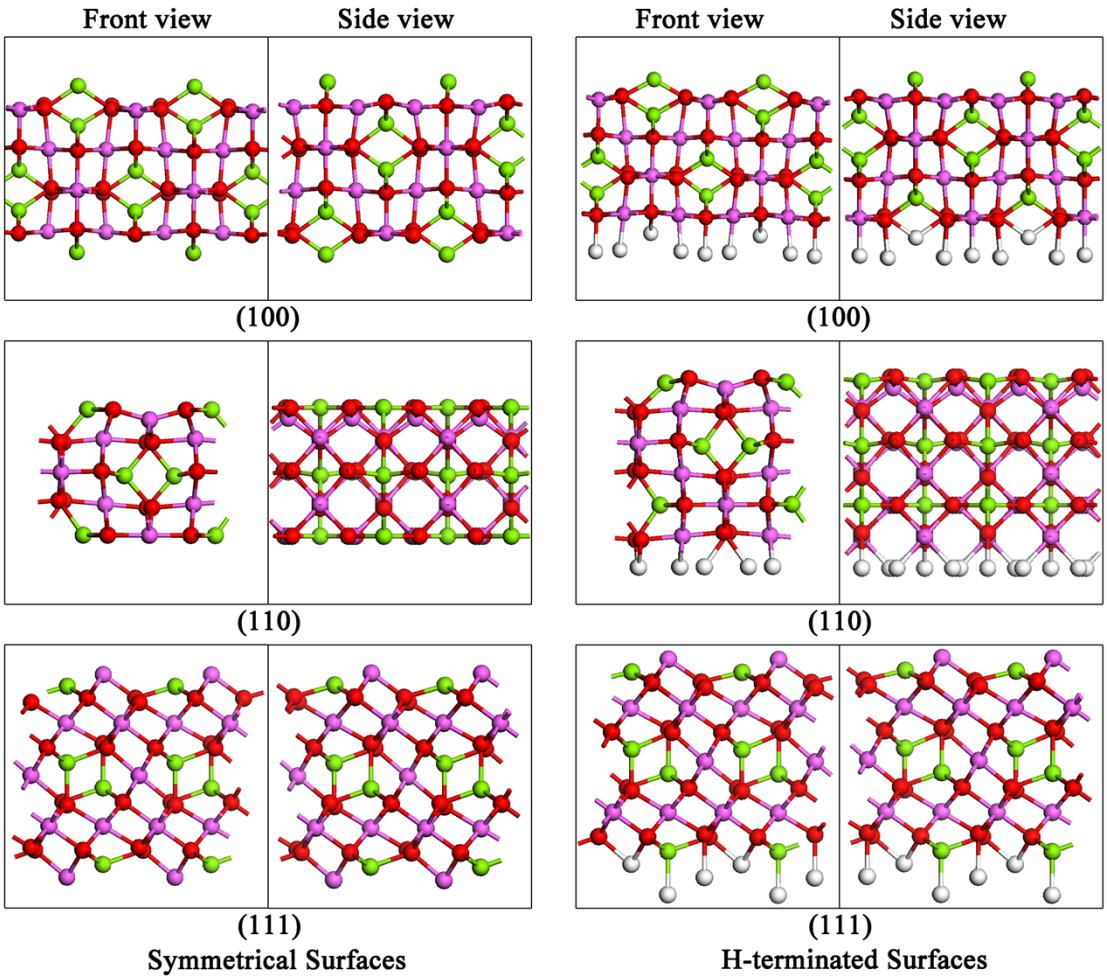

Figure S4. Front and side views of optimized surface structures: non-stoichiometric surface slab with the similar structure of upper and bottom surfaces, surface slab terminated by hydrogen atoms on the bottom layer of $MgAl_2O_4$ polar surface. Color coding: red, O atoms; purple, Al atoms; green, Mg atoms; white, H atoms.

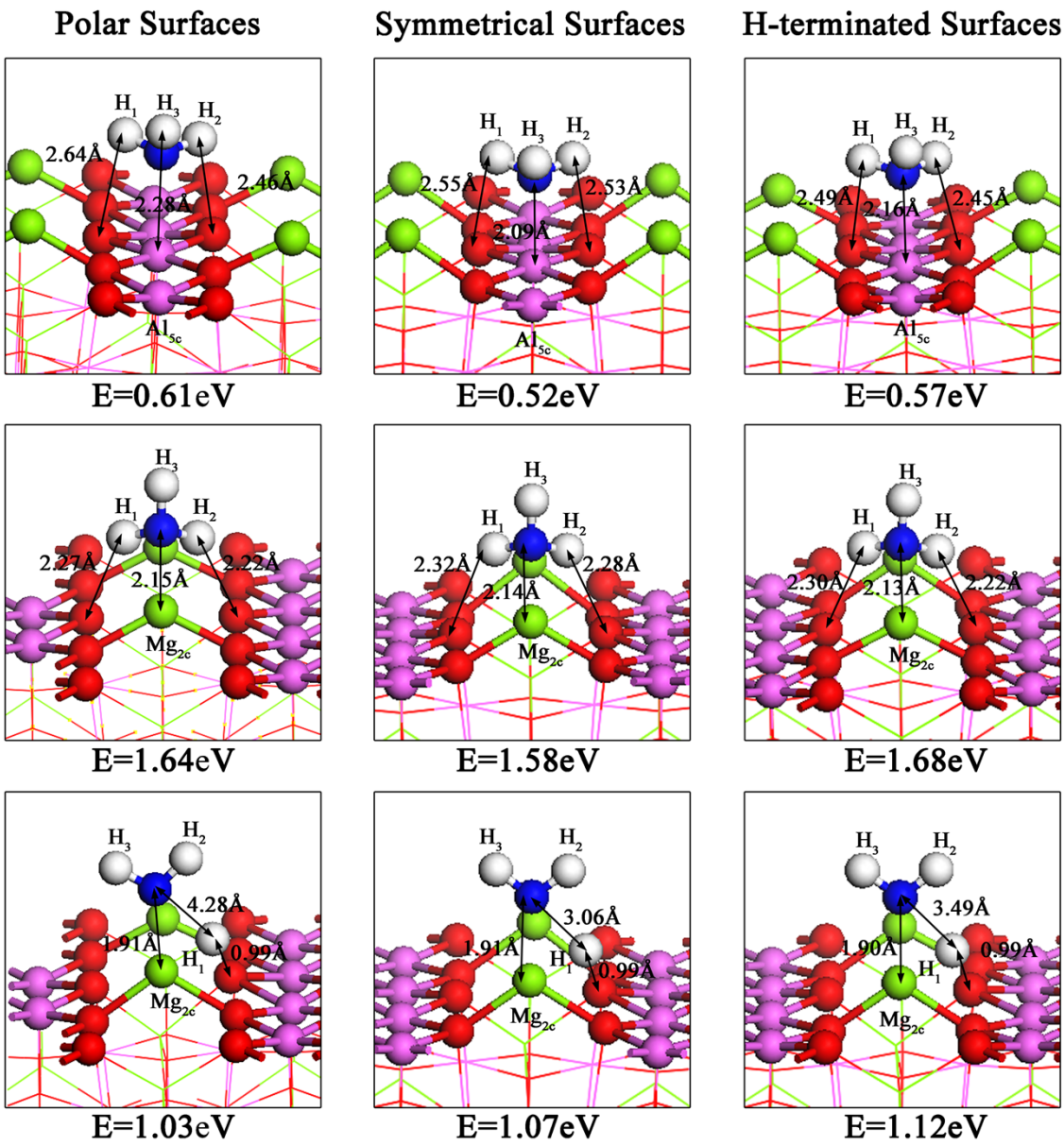

Figure S5. The favorable adsorption configurations and adsorption energies of NH_3 on polar, symmetrical and H-terminated (100) surfaces. Color coding: red, O atom; blue, N atom; white, H atoms.

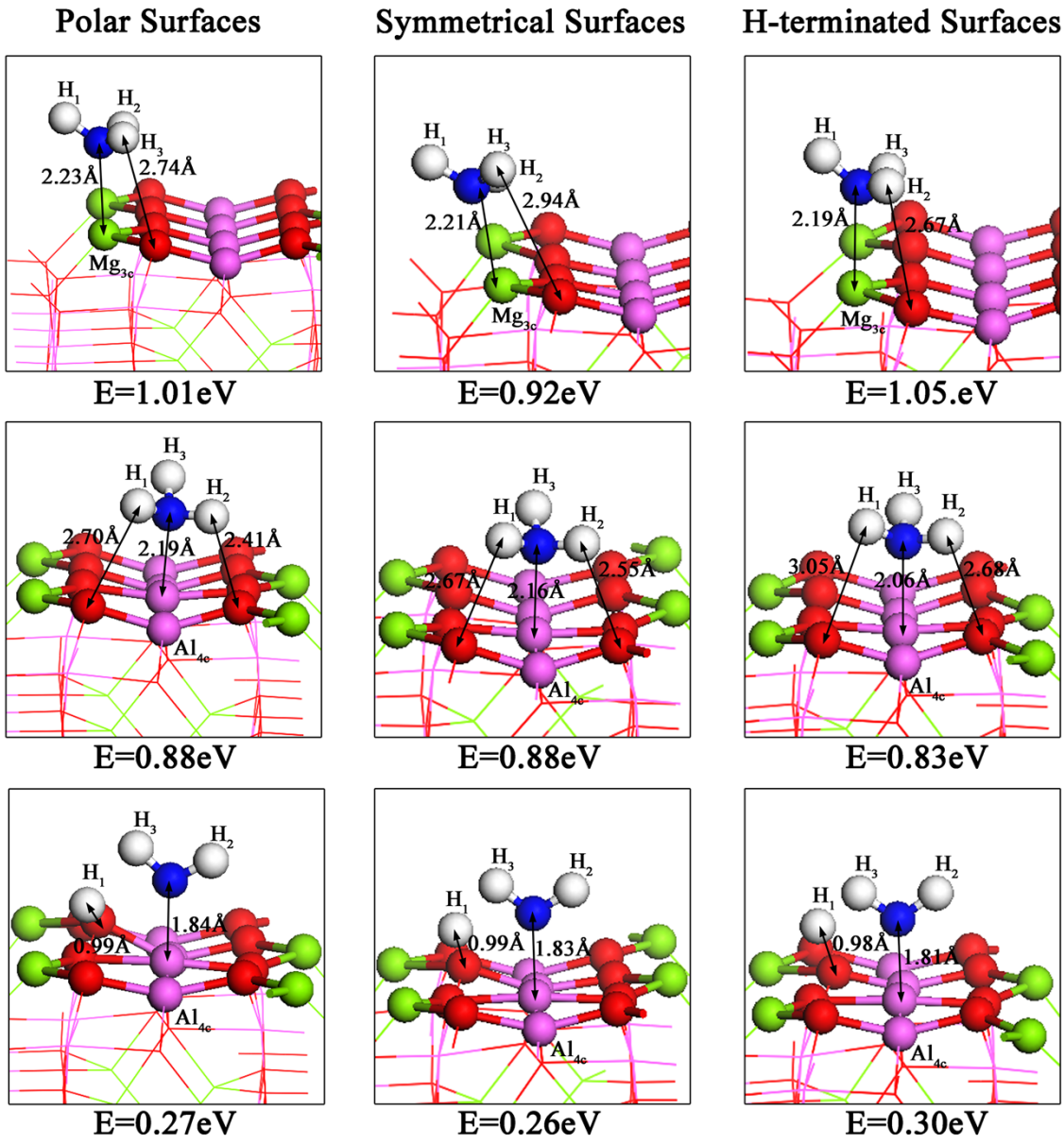

Figure S6. The favorable adsorption configurations and adsorption energies of NH_3 on polar, symmetrical and H-terminated (110) surfaces.

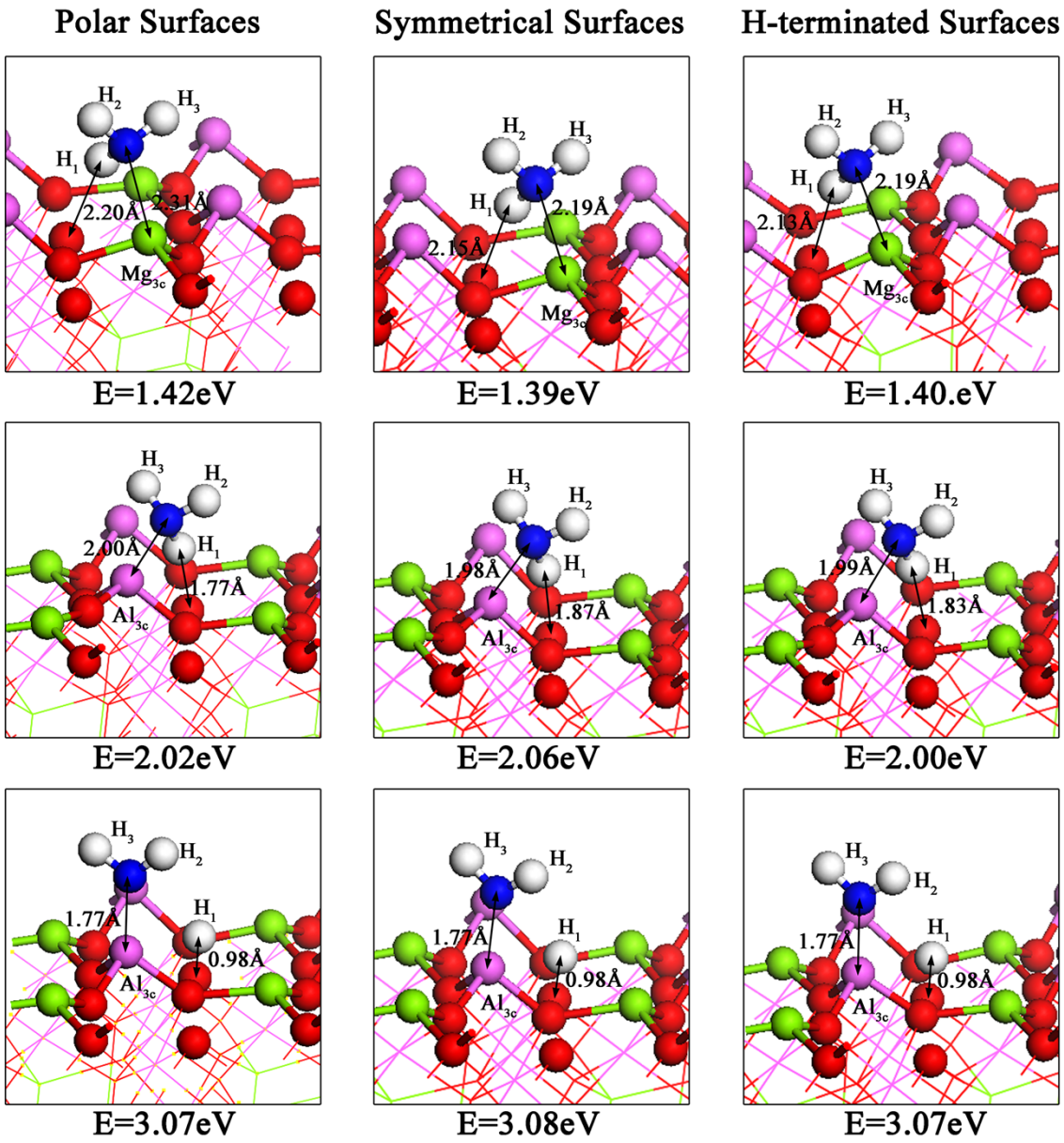

Figure S7. The favorable adsorption configurations and adsorption energies of NH_3 on polar, symmetrical and H-terminated (111) surfaces.

4. The models of oxygen vacancy:

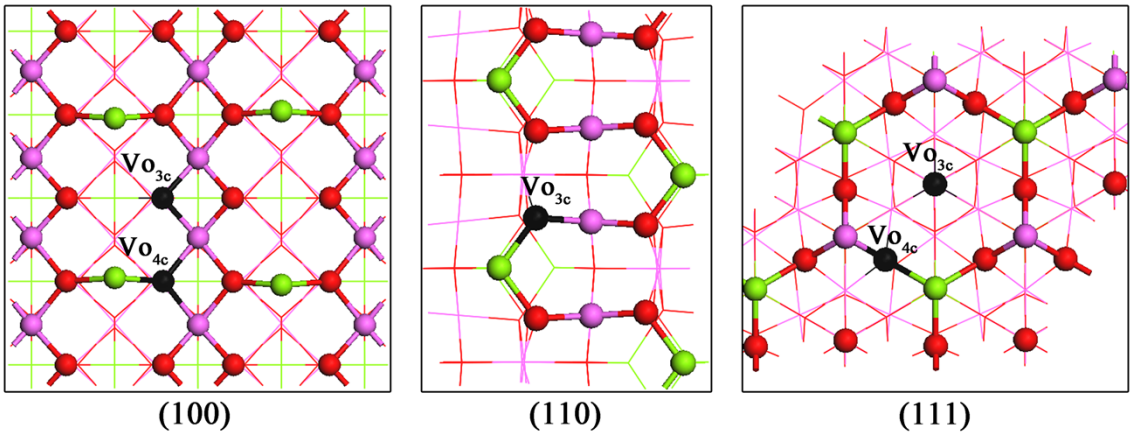

Figure S8. Five configurations of oxygen vacancy on the $MgAl_2O_4$ (100), (110), and (111) surfaces. Color coding: black, O vacancy defect.

5. The configurations of defective surfaces:

The following three Figures below represent the stable configurations of defective (100), (110) and (111) surfaces, and the corresponding adsorption energies are labeled under the structures.

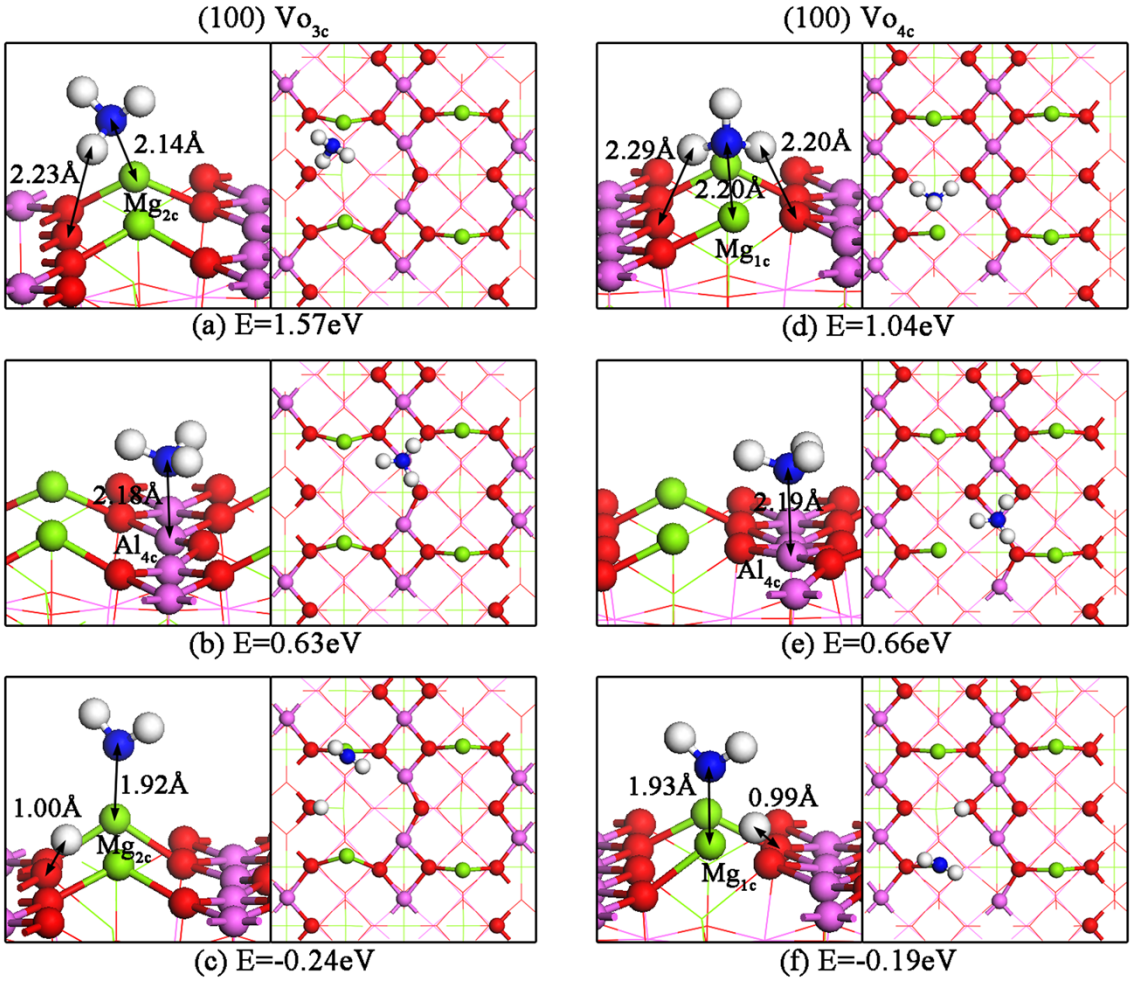

Figure S9. Front and top views of the main adsorption configurations and energies of NH_3 on defective (100) surface. (**a**) H pointed to the O_{3c} atom on Mg_{2c} site of Vo_{3c}; (**b**) the NH_3 pointed to the Al_{4c} atom of Vo_{3c}; (**c**) the dissociation on Mg_{2c} site of Vo_{3c}; (**d**) two H pointed to the O_{3c} atoms on Mg_{1c} site of Vo_{4c}; (**e**) the NH_3 pointed to the Al_{4c} atom of Vo_{4c}; (**f**) the dissociation on Mg_{1c} site of Vo_{4c}.

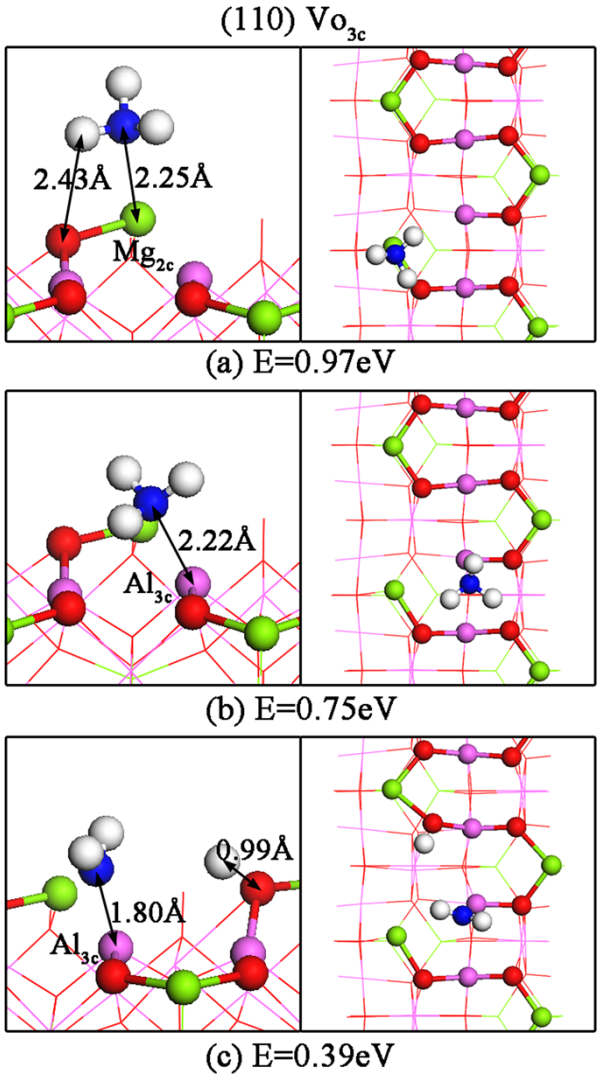

Figure S10. Front and top views of the main adsorption configurations and energies of NH_3 on defective (110) surface. (**a**) H pointed to the O_{3c} atom on Mg_{2c} site of Vo_{3c}; (**b**) the NH_3 located between two Al atoms of Vo_{3c}; (**c**) the dissociation on Al_{3c} site of Vo_{3c}.

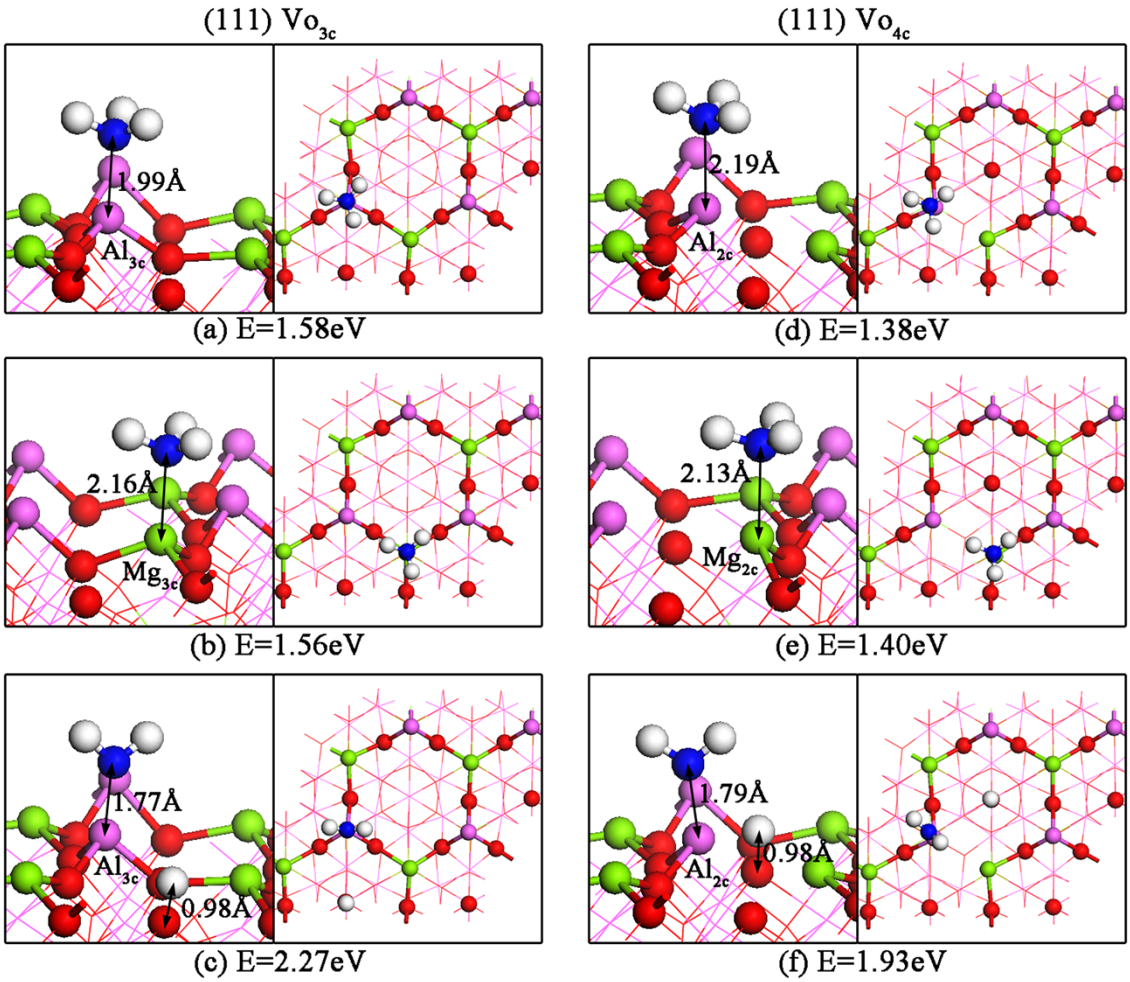

Figure S11. Front and top views of the main adsorption configurations and energies of NH_3 on defective (111) surface. (**a**) the NH_3 pointed to the Al_{3c} atom of Vo_{3c}; (**b**) the NH_3 pointed to the Mg_{3c} atom of Vo_{3c}; (**c**) the dissociation on Al_{3c} site of Vo_{3c}; (**d**) theNH_3 pointed to the Al_{2c} atom of Vo_{4c}; (**e**) the NH_3 pointed to the Mg_{2c} atom of Vo_{4c}; (**f**) the dissociation on Al_{2c} site of Vo_{4c}.